11th International Workshop on Ship and Marine Hydrodynamics
Hamburg, Germany, September 22-25, 2019

A Numerical Investigation of the Turbulent Flow around a Scale Model JBC Hull using the Generalized k-ω (GEKO) Turbulence Model

P.S.Sharkey[1,*], F.R.Menter[2]

[1]ANSYS UK Ltd, Milton Park, Abingdon, England
[2]ANSYS Germany GMBH, Otterfing, Germany

*Corresponding author, patrick.sharkey@ansys.com

ABSTRACT

In this investigation, qualitative comparisons with experimentally obtained PIV data from a scale-model wind tunnel facility are made with numerical solutions obtained using CFD for the Japan Bulk Carrier (JBC) geometry. Distributions of relevant quantities such as local velocity, local vorticity and local turbulence quantities at specific locations in the near-stern region are compared in both straight-ahead and pure-drift configurations.

For the numerical investigation, a new turbulence model, *Generalized k-ω* (GEKO), is employed. This model combines the approach of various other two-equation RANS based models and extends the range of application by providing the user with free parameters (based on near-wall influence, flow separation, mixing, and jet spreading) that can be adjusted for specific types of flow. The effect of varying the separation coefficient, C_{SEP} on the hull wake characteristics of the JBC is examined.

Grid dependence studies for various types of unstructured mesh are also conducted to assess the sensitivity of the results to grid type and grid resolution.

1 INTRODUCTION

The advent and continued progress of Computational Fluid Dynamics (CFD) as a design tool in the ship hydrodynamics industry has allowed an improved understanding of the flow physics for marine applications. However, accurate predictions of experimental drag-resistance data still pose a challenging problem [1][2]. Many fluid aspects play a role in these flows, with accurate flow predictions in the stern region of the ship being one of the main challenges. Specifically, flow separation in this region either in design or off-design conditions can have a significant effect on performance and can lead to undesirable interactions with the propulsion system. Capturing flow separation therefore is a key element of accurate simulations. RANS model separation prediction capabilities also come into play in the optimization of the interaction of the hull boundary layer with the propulsion system [3][4].

It is generally acknowledged that in strongly separated flows, the use of hybrid RANS-LES methods is more reliable than pure RANS computations [5] . However, it is important to keep in mind that in classical hybrid models, the separation onset is still a result of the predictions of the underlying RANS part of the turbulence model. Especially due to the high Reynolds numbers of marine flows, the application of LES/WMLES inside the boundary layers will remain out of reach for the foreseeable future. This necessitates the availability of highly accurate/tuned boundary layer RANS models, both for pure RANS and RANS-LES simulations.

Predicting flow separation under adverse pressure gradients is still a challenging task for RANS models and seems to a degree to be case/application dependent. For example, it is known that for the prediction of the maximum lift coefficient, C_{lmax}, for 2D airfoils, model settings need to be chosen which are very sensitive to separation onset [6], whereas for more general 3D flows, a more conservative model is often desirable. More generally, one could argue that a universal RANS model is unlikely to appear, and as

an alternative approach, flexible turbulence models are needed which can be optimized/calibrated for different types of flows. One such model, termed Generalized k-ω model (GEKO), has recently been developed by ANSYS [7]. It features several free coefficients, which can be tuned by non-turbulence experts, without negatively affecting the basic model calibration for e.g. flat plates and standard free shear flows. It thereby enables CFD practitioners to optimize the turbulence model for their specific application. The coefficients can be tuned globally or through user defined functions zonally/locally. In the future, it is anticipated that the model can also serve as a basis for *machine learning*, by training the free coefficients based on available experimental data and Artificial Intelligence [8].

In the current study, the effect of changing the boundary layer and separation prediction behaviour of the GEKO model will be evaluated for a typical container ship configuration. It will be shown that the boundary layer characteristics and the separation lines can be severely augmented by changing only one of the main model parameters globally. As far as experimental data are available, the effect of these parameter changes compared to data will be demonstrated. As the GEKO model is not fully published, the current investigation can only provide an impression on the effectiveness of the GEKO concept and not on the details. Still, it is hoped that the comparisons show the power of this conceptual modelling approach.

2 WIND TUNNEL ANALYSIS OF THE JAPAN BULK CARRIER

The Japan Bulk Carrier (JBC) hull is a capesize bulk carrier equipped with a stern duct as an energy saving device. The JBC was introduced as a design concept at the Tokyo 2015 Workshop on CFD in Ship Hydrodynamics, where several CFD studies were undertaken by participants and compared with LDV data obtained from wind tunnel experiments at the Technical University of Hamburg-Harburg (TUHH). Data used for comparison in this paper has been obtained from more recent experiments using Particle Image Velocimetry (PIV) by Professor Abdel Maksoud's group at TUHH [9]. Details of the wind tunnel facilities and stereoscopic PIV measurement system used for the experimental data collection are detailed on the TUHH website ([10]). A 1/79.7 scale model of the JBC in a twin-hull configuration was used to obtain the PIV data in the wind tunnel.

Figure 1 shows the scale model situated in the wind tunnel at TUHH, and a schematic of the geometry. In this version, the propeller(s) and energy saving device(s) are omitted, but the propeller shaft hubs (bosses) are retained.

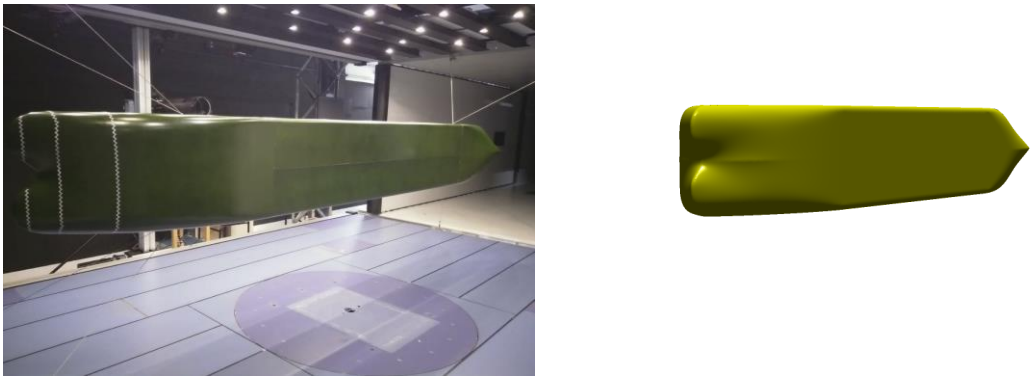

(a) (b)

Figure 1: Geometry for the JBC hull (a) wind tunnel facility at TUHH, (b) CFD surface model

Figure 2 shows the dimensions of the scale model used, including the locations of the *forward perpendicular* (FP) and *aft perpendicular* (AP). The total length of the model is 3651 mm, with a width of 565 mm and twin hull height of 415 mm.

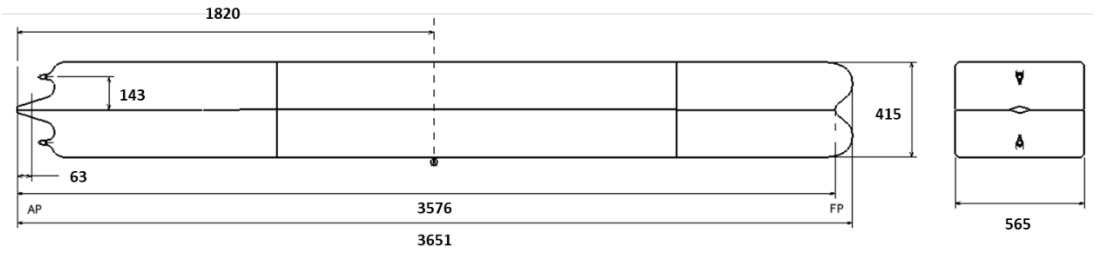

Figure 2: Dimensions (in mm) of JBC tine hull scale model

2.1 Measurement locations

PIV data was obtained at specific planes in the aft region of the hull. Figure 3 shows the locations of the planes relative to the hull geometry.

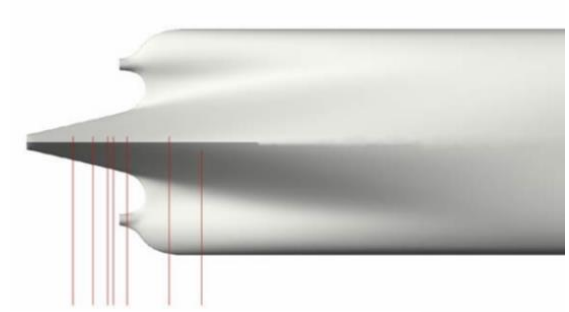

Figure 3: Location of the measurement planes on the JBC hull model

The definition of the plane locations S1 to S7 is described in Table 1. The planes are located upstream of the reference AP, up to a distance of 5% of length between perpendiculars (LP or Lpp). Data is obtained in in both *straight-ahead* and *pure-drift* modes. In pure-drift mode, the model is rotated by 8 degrees to the incoming flow about its central suspension point. Also, for the pure-drift case, the measurement planes are rotated in-line with the rotation of the hull so that the relative locations remain fixed.

Table 1: PIV measurement plane locations

Plane	**Name**	**X_s [mm]**	**X_s/L_{pp}**
S1	SS1/2	175.7	0.0500
S2	SS3/8	131.7	0.0375
S3	Duct mid-chord	74.3	0.0211
S4	Between propeller and duct	55.2	0.0157
S5	Generator line 0.7R	47.8	0.0136
S6	Between A.P. and propeller	27.1	0.0077
S7	A.P.	0	0.0000

3 NUMERICAL MODELING

3.1 Computational domain

The numerical set up has been developed to mimic as far as possible the conditions in the experimental wind tunnel at TUHH.

The computational domain and boundary conditions are shown in Figure 2. The JBC hull model is suspended centrally in a rectangular wind tunnel. Upstream and downstream of the model hull, the wind tunnel is fully enclosed (except for the inlet and outlet) and wall boundary conditions are imposed. A fixed velocity bulk inlet boundary condition (U_b) of 10 m/s is imposed at the wind tunnel model inlet, equivalent to a Reynolds number of 2.42 x 10^6 based on the length between perpendiculars (LP). A fixed pressure outlet condition was imposed at the outlet end of the tunnel (0 Pa). The central portion of the wind tunnel model contains an outlet boundary condition which is designed to replicate the observation window through which experimental data is obtained during the tests.

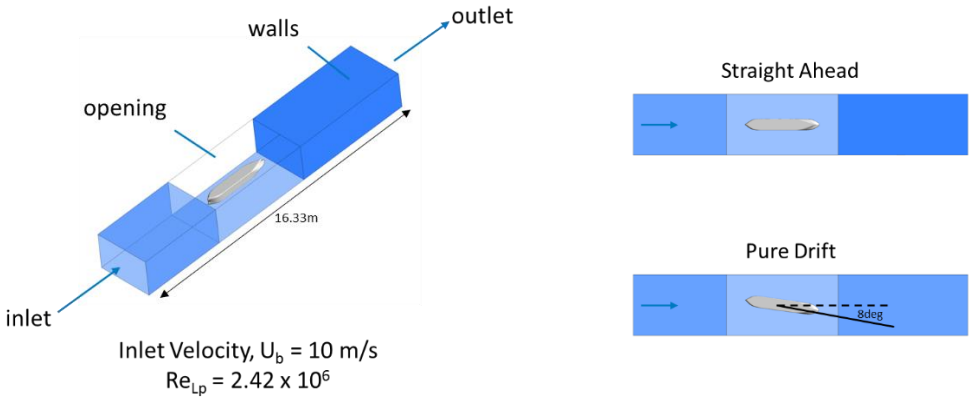

Figure 4: Computational domain and boundary conditions for the straight ahead and pure drift cases

Both *straight-ahead* mode (hull normal to incoming flow) and *pure-drift* mode (hull oblique to incoming flow) were simulated. For the pure drift case, the model is rotated about its central suspension point to provide an oblique angle of the flow to the hull of 8 degrees. The orientation of the model with respect to the global coordinate system is such that X is the flow direction and Y the crossflow direction.

3.2 The GEKO Turbulence Model

The GEKO model is developed to consolidate the advantages of many available 2-equation eddy-viscosity based RANS models into a single, unified, general purpose model to accommodate a wide range of flow conditions and applications [7]. It is based on a *k-ω* model formulation and reads as follows:

$$\frac{\partial(\rho k)}{\partial t}+\frac{\partial(\rho \bar{U}_j k)}{\partial x_j}=P_k-C_\mu \rho k\omega+\frac{\partial}{\partial x_j}\left(\left(\mu+\frac{\mu_t}{\sigma_k}\right)\frac{\partial k}{\partial x_j}\right) \quad (1)$$

$$\frac{\partial(\rho \omega)}{\partial t}+\frac{\partial(\rho \bar{U}_j \omega)}{\partial x_j}=C_{\omega 1}F_1\frac{\omega}{k}P_k-C_{\omega 2}F_2\rho\omega^2+\rho F_3 CD+\frac{\partial}{\partial x_j}\left(\left(\mu+\frac{\mu_t}{\sigma_\omega}\right)\frac{\partial \omega}{\partial x_j}\right) \quad (2)$$

where $\mu_t=\rho\upsilon_t=\frac{k}{\max(\omega,S/C_{realize})}$, $P_k=-\tau_{ij}\frac{\partial \bar{U}_j}{\partial x_j}$, $CD=\frac{2}{\sigma_\omega}\frac{1}{\omega}\frac{\partial k}{\partial x_j}\frac{\partial \omega}{\partial x_j}$, $C_{realize}=\frac{1}{\sqrt{3}}$

In addition to the basic coefficients, also present in other two-equation models, the GEKO model features additional 'free' parameters which can be adjusted to cover a wide range of flow variations. These coefficients, implemented through the functions F_1, F_2 and F_3 in the above equations, are designed to control specific physical aspects of the model, namely: near wall behaviour; separation; free jet dynamics; secondary flows at corners; effects of curvature; free stream mixing.

In this paper the effects of varying the separation coefficient, C_{SEP}, have been investigated, as it directly affects the separation prediction and is therefore expected to have the strongest impact on the flow in the stern and the wake region of the JBC hull. Note that the setting C_{SEP}=1 (and all other parameter defaults) corresponds to an exact transformation of the standard k-ε model to a k-ω formulation (augmented by a realizability limiter with $C_{realize}$=0.577 to avoid stagnation build-up of turbulence). The setting C_{SEP}=1.75 is a close approximation of the SST model in terms of its separation prediction characteristics (but not an exact transformation of that model). Larger values of C_{SEP} will result in earlier and stronger separation compared to smaller values.

3.3 Mesh generation

Both unstructured tetrahedra and polyhedra were used to discretize the computation domain. The resulting meshes use prism layers extruded from the surface discretization of the hull body to capture near-wall boundary effects. Care was taken to ensure that the integrity of the surface was retained by enabling curvature preserving meshing, as well as ensuring sufficient number of prism layers were created around the hull body. Volume mesh refinement at the stern and in the wake was used to resolve wake vortices and turbulence. Depictions of the meshes used at relevant location in the domain and on the hull surface are shown in Figures 5 and 6.

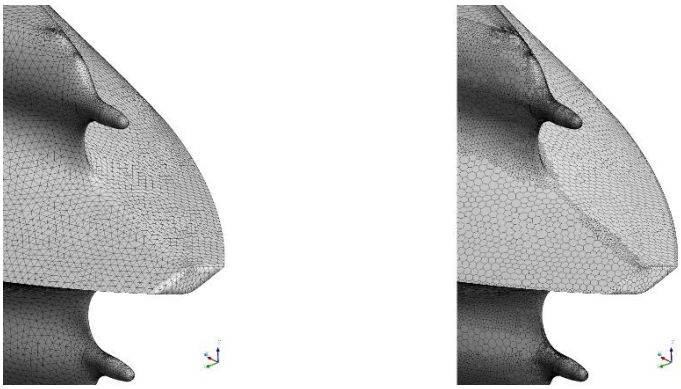

Figure 5: Fine Tetrahedral and Polyhedral meshes on hull body stern

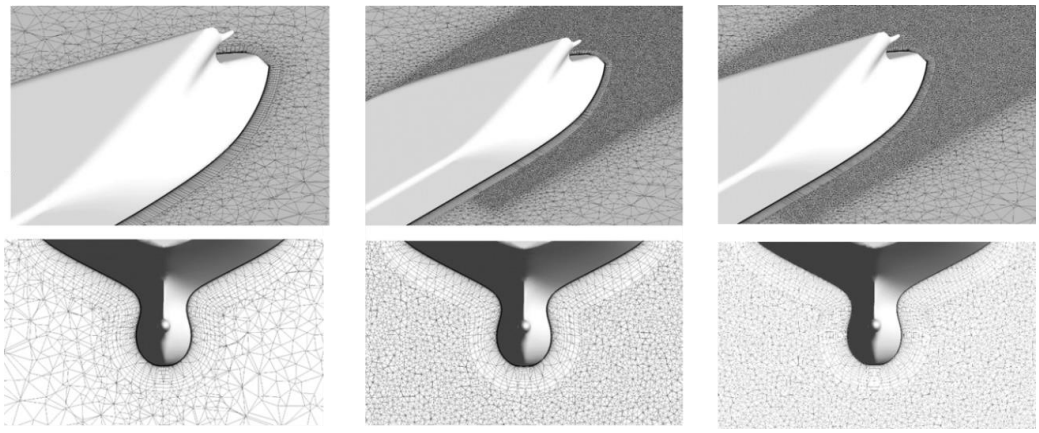

(a) 5.18M cells (b) 13.31M cells (c) 16.86M cells

Figure 5: Coarse, medium and fine prism-tetrahedral meshes created for the JBC hull on the symmetry plane and Plane S1

3.4 Discretization and solution

All simulations in this investigation were conducted with ANSYS Fluent®, a generalized, commercial finite volume CFD code capable of solving flows on structured and unstructured meshes comprising various cell types including hexahedra, tetrahedra and general polyhedra. 2nd order spatial discretization for the pressure, momentum and turbulence equations was used, with a least squares cell-based method for the gradient formulations.

Solution of the discretized equations was accomplished with ANSYS Fluent®'s coupled solver operating in pseudo-transient mode, using a pseudo-timestep automatically calculated based on the global flow timescales, and appropriate convergence criteria. An isothermal, incompressible material, based on air at standard temperature pressure, was used as the working fluid with properties adjusted to achieve the desired Reynolds number.

4 RESULTS

4.1 Boundary layer profiles

Velocity profiles at specific locations on the hull were compared with experimental data to determine the adequacy of the near-wall mesh resolution. These are plotted in Figure 7.

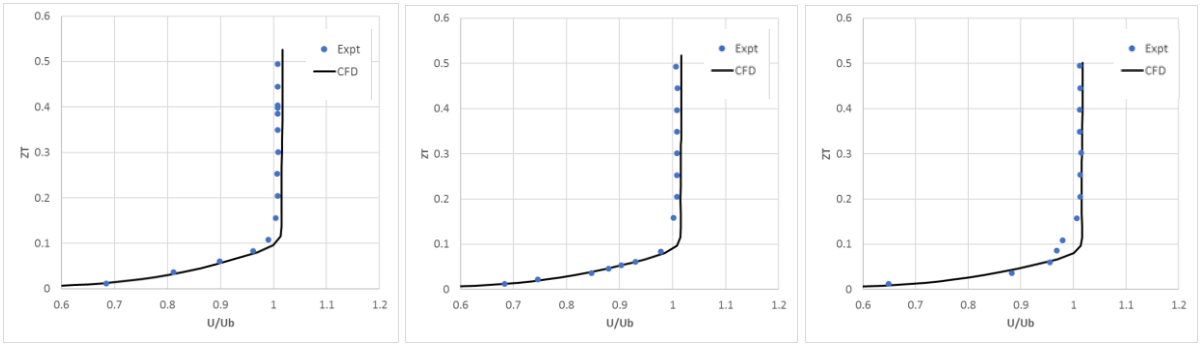

(a) x/L_{pp} = 0.5 (b) x/L_{pp} = 0.55 (c) x/L_{pp} = 0.6

Figure 7: Non-dimensional velocity profiles, U/U_b, at three locations in the near wall region for the straight-ahead case (16.86M Tetrahedral)

The boundary layer profiles, plotted against non-dimensional distance from the wall ZT (where ZT = z/HT and where HT is the half-hull height), show that the resolution of the mesh near the wall adequately captures the velocity gradient and that the overall match with the experimental measurements is very good. At these locations (essentially from halfway along the hull) the boundary layer is fully developed and quite thick; a value of ZT = 0.1 is equivalent to 10% of the half-hull height.

4.2 Qualitative comparisons with experimental PIV measurements at sectional planes

For the discussion of the impact of changes to the GEKO parameter C_{SEP}, it is important to first illustrate its effect for a simple generic flow, like the CS0 diffuser [11]. In the CS0 case, a boundary layer on an axisymmetric body undergoes an adverse pressure gradient leading to a shallow separation and downstream reattachment. Figure 8 shows the velocity profiles as computed with different values for the C_{SEP} coefficient. Note again that a value of C_{SEP}=1.0 corresponds to an exact transformation of the k-ε model to a k-ω formulation. A value of C_{SEP}=1.75 corresponds approximately to the performance of the SST model. As seen from

Figure 8, the GEKO model covers a wide range of flow calibrations, from firmly attached flow for C_{SEP}=0.7, to a significant over-separation for C_{SEP}=2.5. This is also the permissible parameter space for this coefficient.

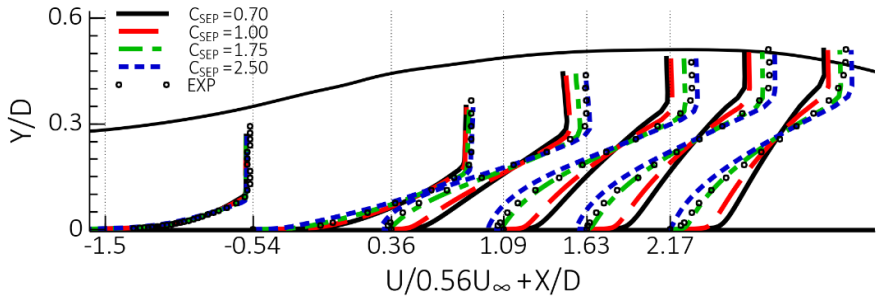

Figure 8: Impact of variation in CSEP on velocity profiles for CS0 diffuser flow [11]

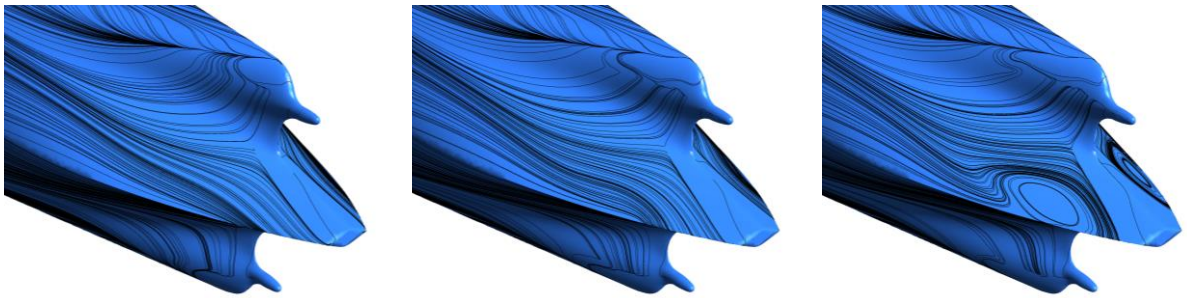

(a) C_{SEP}=1.0 (b) C_{SEP}=1.75 (c) C_{SEP}=2.5

Figure 9: Wall streamlines for the straight-ahead case for different values of C_{SEP}

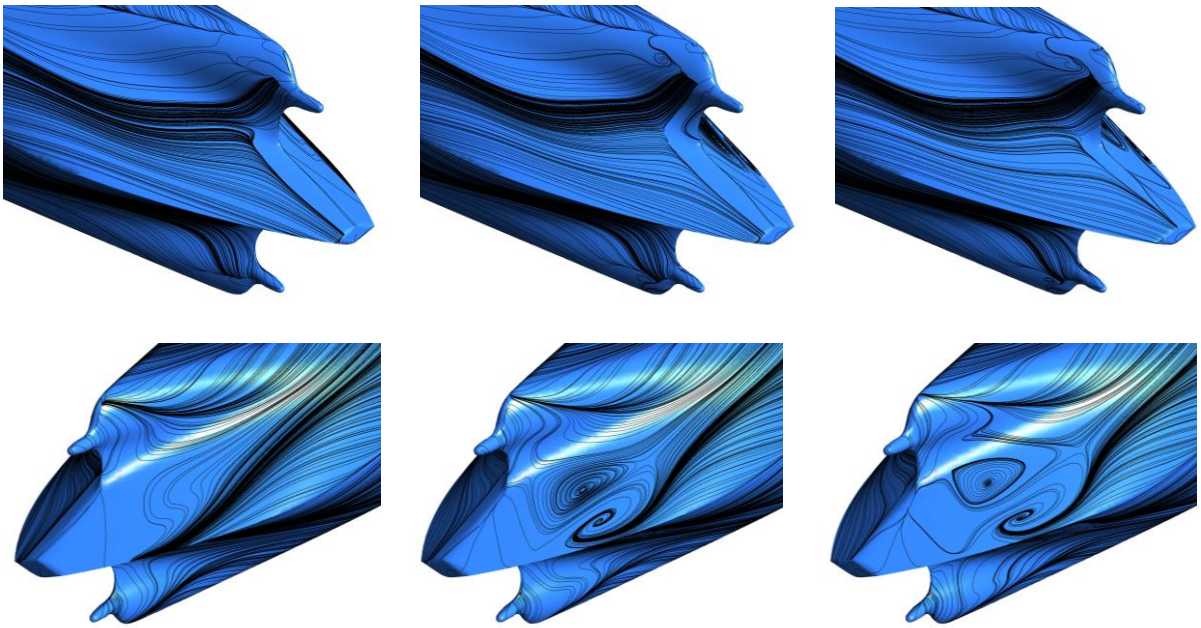

(a) C_{SEP}=1.0 (b) C_{SEP}=1.75 (c) C_{SEP}=2.5

Figure 10: Wall streamlines for the pure-drift case for different values of C_{SEP}.
(top: Leeward side, bottom: Windward side)

Figure 9 shows the wall streamlines in the stern region of the hull for the straight-ahead case for the three values of C_{SEP} (1.0, 1.75, 2.5). The separation line can be substantially modified with this simple model parameter change, allowing for a large calibration space for such flows and the effect of increasing the parameter can be clearly seen in the streamlines . Figure 10 shows the same variation in C_{SEP} for the pure drift case, both on the leeward and the windward side of the hull. As expected, flow heavily separated on the leeward side however the separation is effectively fixed by the geometry, and because of this the effect of varying C_{SEP} is small. The effect is more apparent, however, on the windward side when increasing C_{SEP} from 1.0 to 1.75, although the degree to which the separation lines have been changed when increasing C_{SEP} further to 2.5 appears to be small. Unfortunately, no experimental oil flow pictures exist for the current experiment, so that the comparison can only be performed between the numerical results. However, the impact of changes in C_{SEP} can clearly be seen.

Figures 11 and 12 show comparisons of X velocity solutions at different mesh resolutions (detailed in Figure 5) at Planes S4 and S7 (AP) for the straight-ahead case using default GEKO parameters, which is closest to SST. Comparison with the experimental PIV data shows a good qualitative match, whilst increasing mesh resolution from coarse to fine produces some improvements in solution away from the hull compared to the experimental data.

Figure 13 shows PIV data for non-dimensional X velocity at the AP compared to solutions obtained with tetrahedral and polyhedral meshes for cases with C_{SEP}=1.0. The solutions show small differences in velocity component distribution, and results for other quantities (not shown here) exhibit similar small differences, but overall the solutions are very similar. The major advantage in using polyhedral meshes is the ability to capture similar flow resolutions for lower cell counts (the polyhedral mesh for this case contains approximately half the number of cells compared to the tetrahedral mesh), providing better performance in terms of speed.

Figure 14 shows comparisons for non-dimensional X velocity, U_x/U_b, at Plane S1. The simulation results are generally in line with the PIV data for all three values of C_{SEP} with neither high nor low values showing any greater propensity to capture the wake details on the leeward side to any greater accuracy. At the AP, however, the effects of varying C_{SEP} become more apparent; increasing the parameter produces a wider wake on the windward side. It is arguable whether the distribution is a better match for C_{SEP} =1.75 or C_{SEP} = 2.5, as whilst the wake width is a better match for a value of 1.75, other features in the wake compare slightly better for a value of 2.5. For other velocity component distributions (Figures 15 and 16), the picture is less clear as there is little difference in solutions with low or high C_{SEP} either at plane S1 or plane S7, though the predictions of these quantities compare very well with experiment.

The picture is different again when viewing contours of non-dimensional vorticity, $\omega_x/(U_b/Lpp)$, in Figure 14. Here, the best comparison is arguably made with values of C_{SEP} between 1.0 and 1.75.

In Figure 18, the distributions of non-dimensional turbulence kinetic energy, TKE/U_b^2, are reasonably consistent with the PIV data at Plane S1, although higher levels of turbulence are present just off the hull surface; measurements at plane S7 (AP) show reduced levels of turbulence and a distribution consistent with the upstream measured levels at Plane S1. The simulation result, however, is significantly different: not only are the distributions different, levels are generally higher at Plane S7 than at Plane S1, with significantly more turbulence being generated in the mid-plane of the hull. By contrast, the same quantity plotted on planes S4 and S7 for the straight-ahead case (Figure 19) show levels and distributions that are reasonably consistent. However, both comparisons are hampered slightly by the fact that the PIV image is somewhat distorted and a direct comparison by eye is difficult.

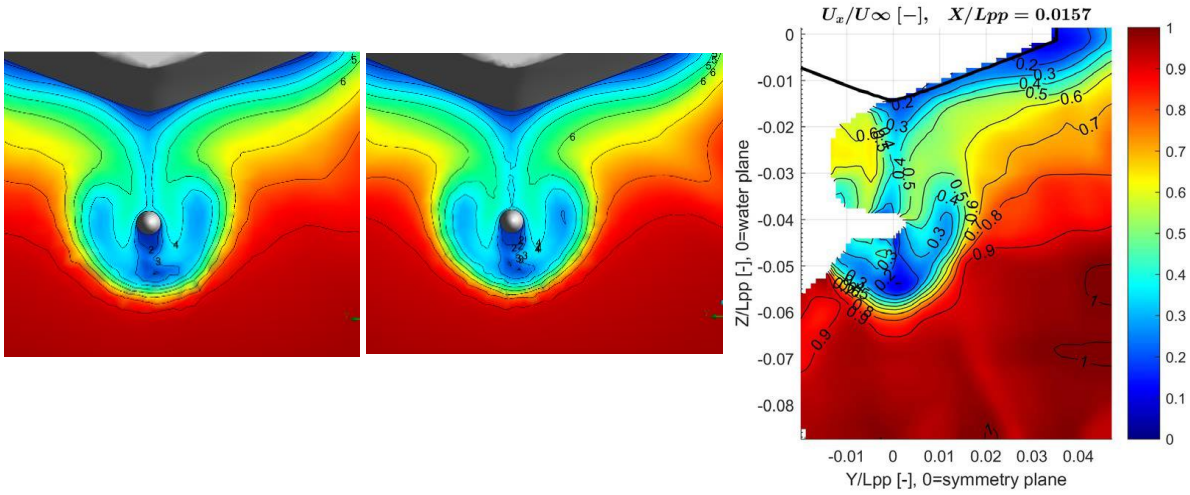

(a) (b) (c)

Figure 11: Contours of non-dimensional X velocity (U_x/U_b) at Plane S4 for the straight-ahead case with default GEKO parameters: (a) Coarse Tetrahedral Mesh, (b) Finest Tetrahedral Mesh, (c) PIV

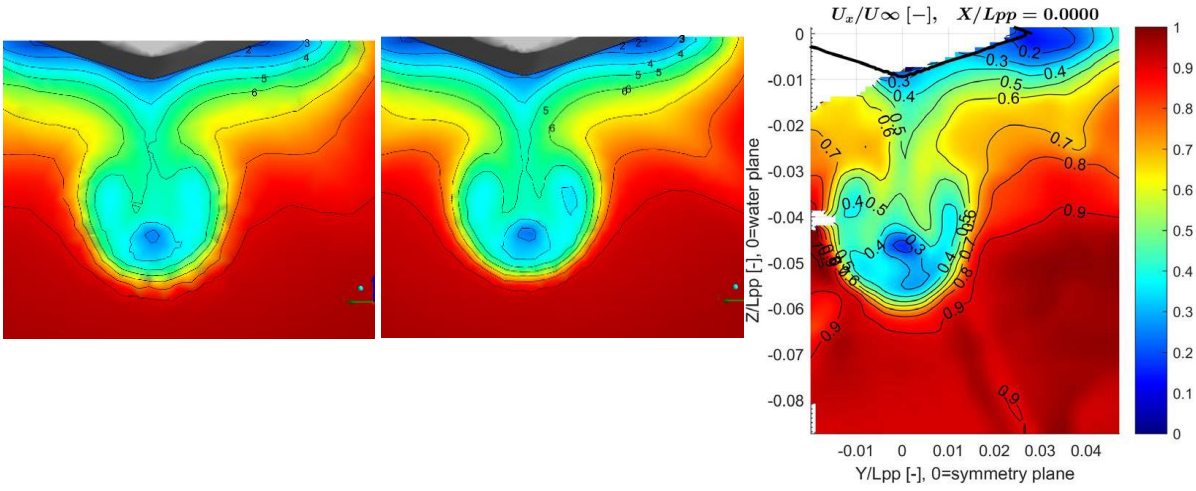

(a) (b) (c)

Figure 12: Contours of non-dimensional X velocity (U_x/U_b) at Plane S7 (AP) for the straight-ahead case with default GEKO parameters: (a) Coarse Tetrahedral Mesh, (b) Finest Tetrahedral Mesh, (c) PIV

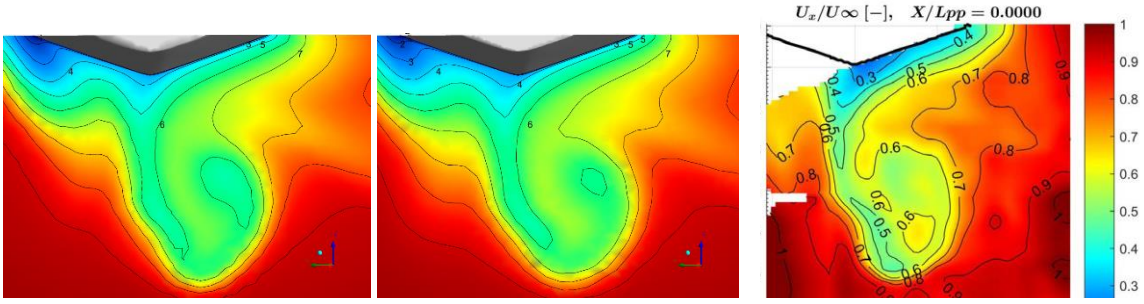

(a) (b) (c)

Figure 13: Contours of non-dimensional X velocity (U_x/U_b) at Plane S7 for the pure-drift case with C_{SEP}=1.0: (a) Tetrahedral solution, (b) Polyhedral solution, (c) PIV

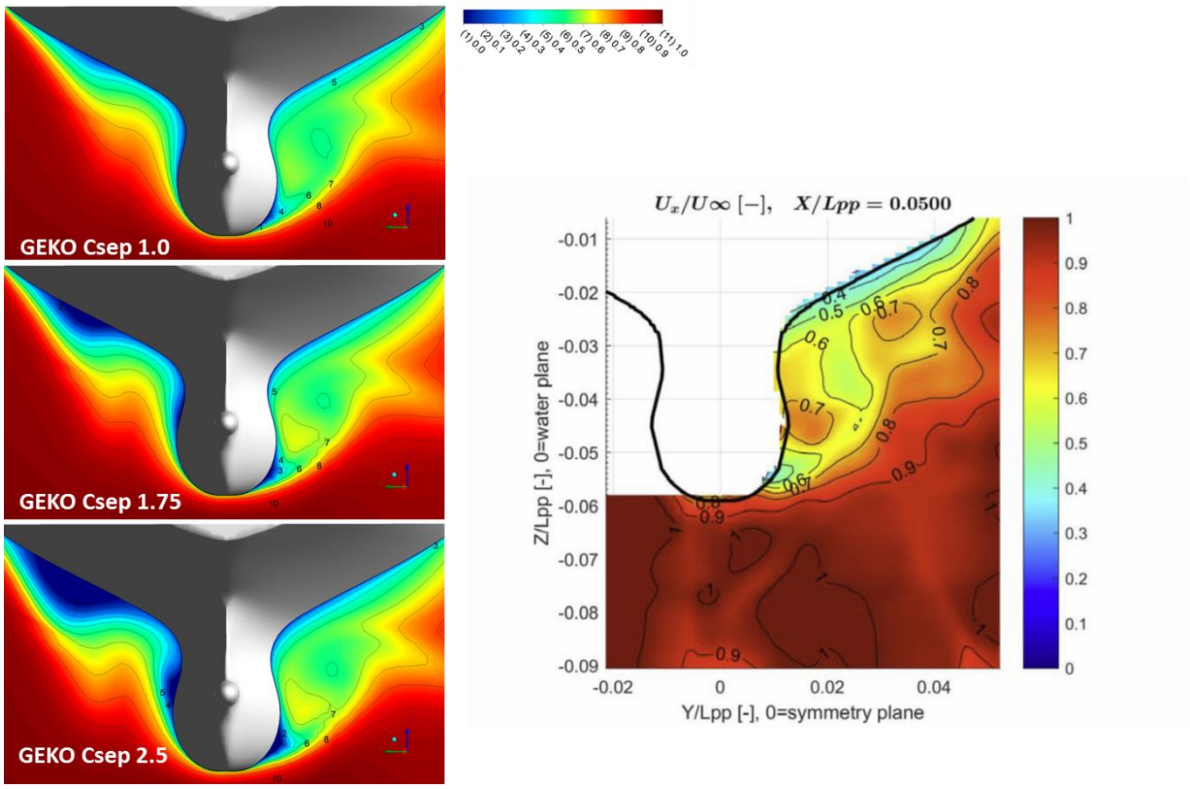

(a) U_x/U_b Plane S1

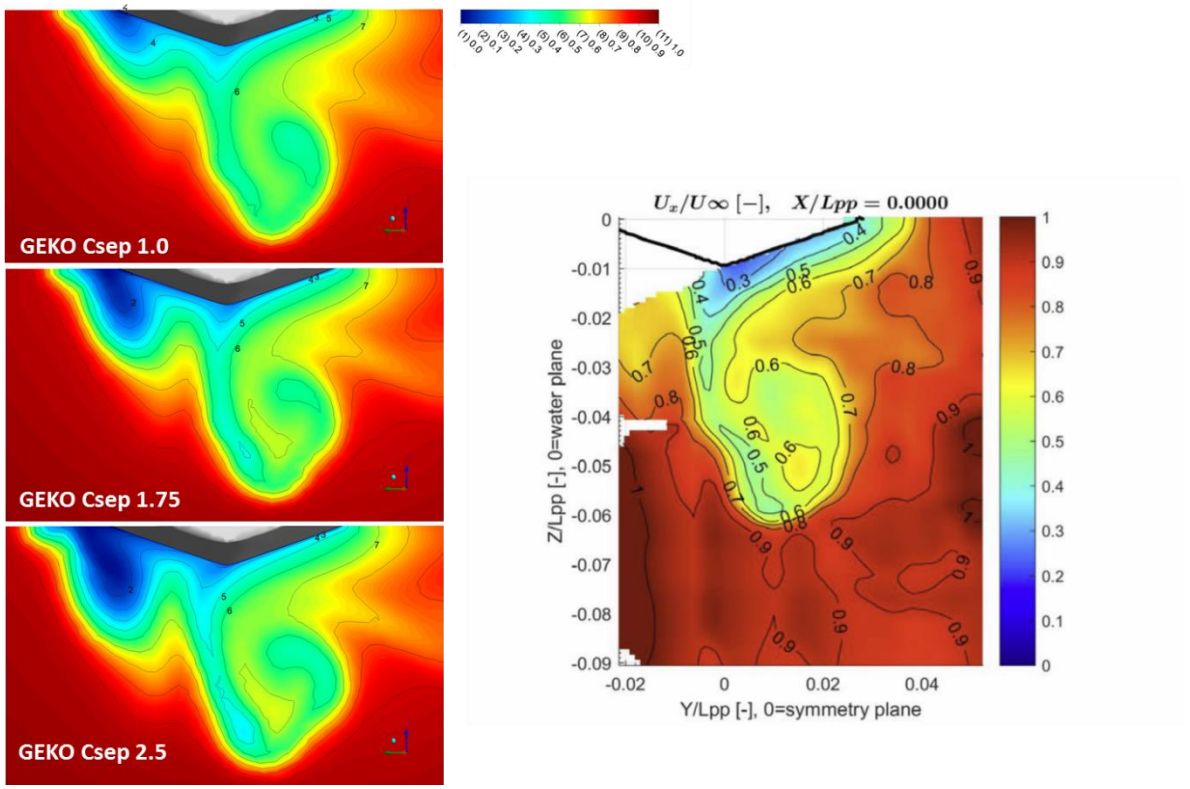

(b) U_x/U_b Plane S7 (AP)

Figure 14: Contours of non-dimensional X velocity (U_x/U_b)

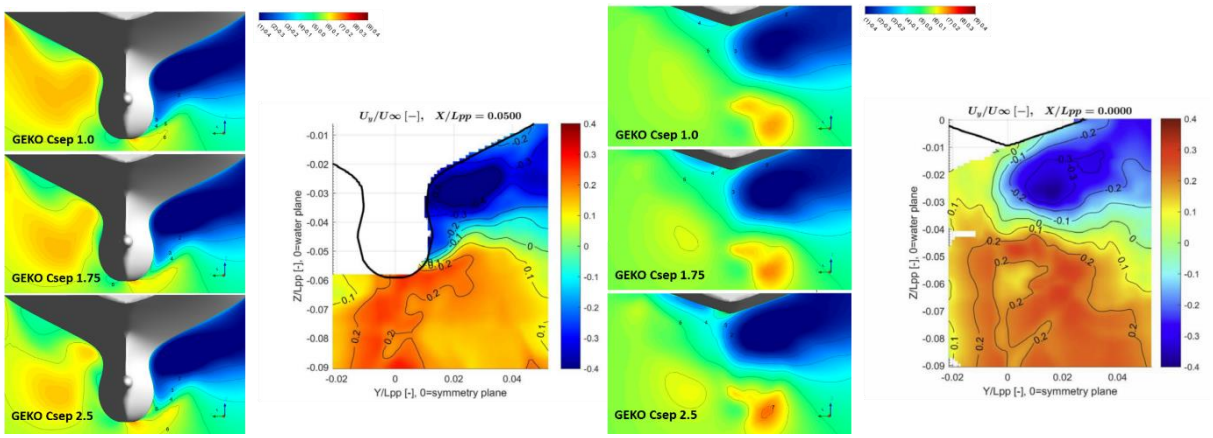

(a) Plane S1 (b) Plane S7 (AP)

Figure 15: Contours of non-dimensional Y velocity (U_y/U_b)

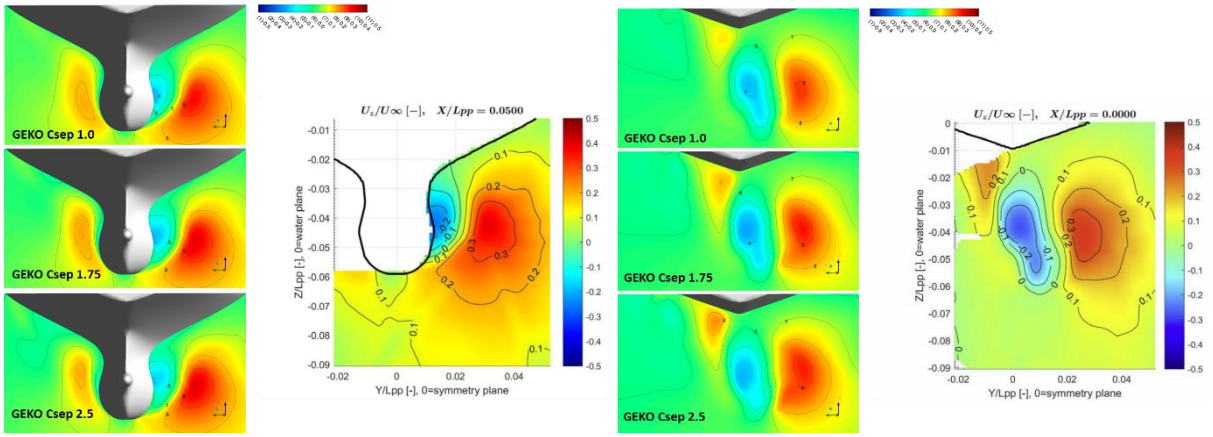

(a) Plane S1 (b) Plane S7 (AP)

Figure 16: Contours of non-dimensional Z velocity (U_z/U_b)

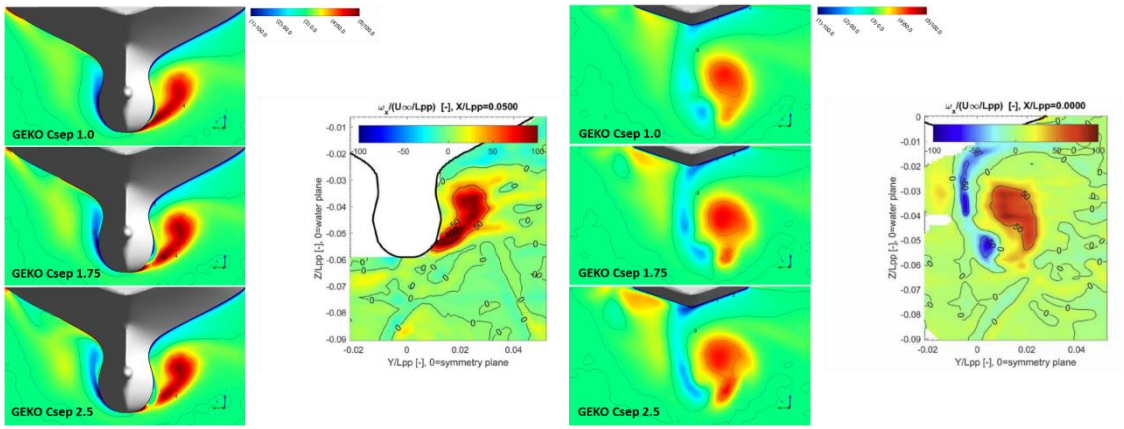

(a) Plane S1 (b) Plane S7 (AP)

Figure 17: Contours of non-dimensional X vorticity ($\omega_x/(U_b/L_{pp})$)

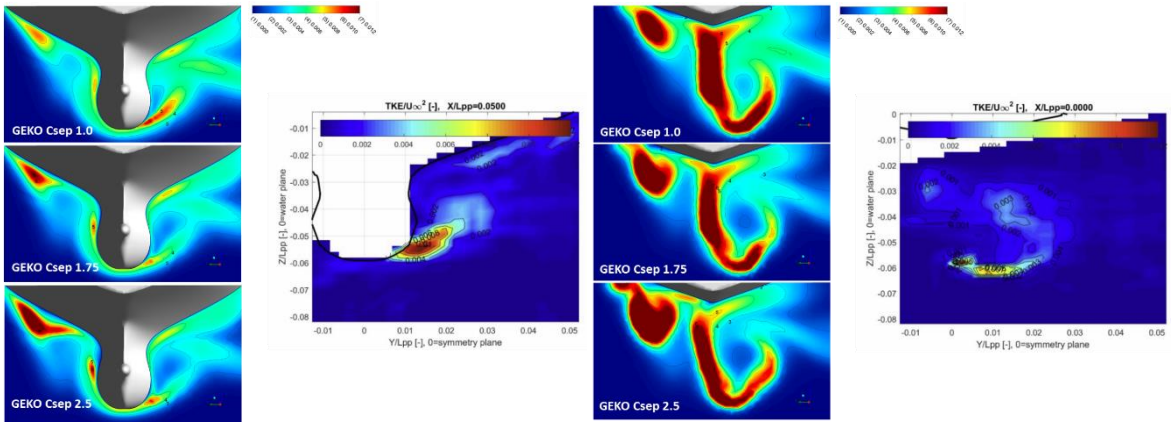

(a) Plane S1 (b) Plane S7 (AP)

Figure 18: Contours of non-dimensional turbulence kinetic energy (TKE/U_b^2) for the pure-drift case

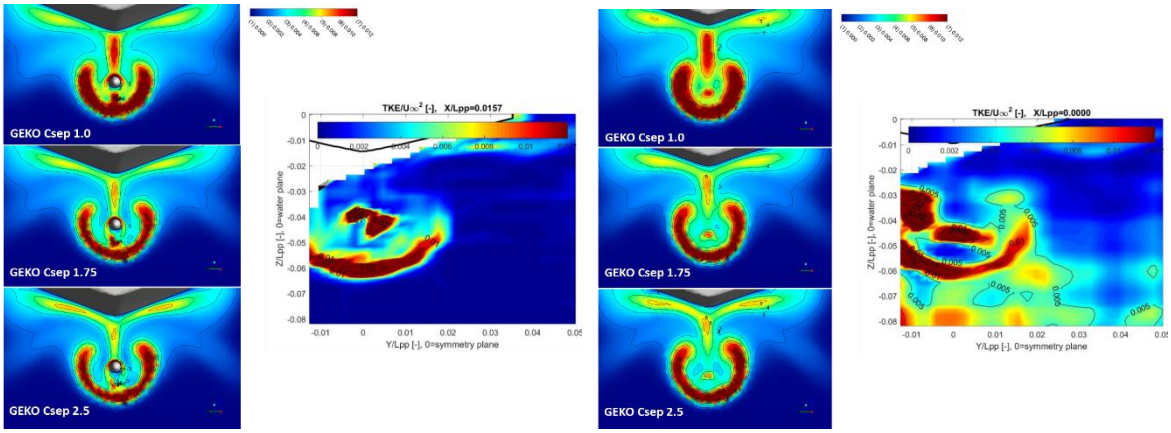

(a) Plane S4 (b) Plane S7 (AP)

Figure 19: Contours of non-dimensional turbulence kinetic energy (TKE/U_b^2) for the straight-ahead case

5 CONCLUSION

The GEKO turbulence model has been applied to the Japan Bulk Carrier (JBC) simulation. The versatility of the model with respect to separation prediction has been demonstrated, by changing the main boundary layer parameter C_{SEP} in the model. It has been shown that the separation location and strength can be modified without expert turbulence knowledge over a substantial range. A detailed calibration of the model would require more detailed information on the flow separation location, best in the form of oilflow pictures. It should be noted also that the GEKO model can be combined with nonlinear stress-strain models, full Reynolds Stress Models as well as hybrid RANS-LES methods for improved predictions of the strongly separated flow regions downstream of the separation line.

ACKNOWLEDGEMENTS

The authors would like to thank Professor Moustafa Abdel-Maksoud and Mr Ahmed Sahab at TUHH for providing experimental data for the JBC hull model, and for providing help and guidance on the configuration of the wind tunnel facilities relevant to the numerical modelling.

REFERENCES

[1] Jasak, H., Vukcevic, V. and Lalovic, I. (2018): "CFD Validation and Grid Sensitivity Studies of Full Scale Ship Self Propulsion, International Journal of Naval Architecture and Ocean Engineering (2018) 1-11.

[2] Rahaman1, M.M, Islam, M., Islam, T, and Khondoker, R.H. (2017), "Calm Water Resistance Prediction of a Bulk Carrier using Reynolds Averaged Navier-Stokes Based Solver", AIP Conference Proceedings, Volume 1919, Issue 1, 10.1063/1.5018556

[3] Badoe et al. (2015), "RANS computations of flow around a bulk carrier with energy saving device", Proceedings Tokyo 2015 Ship Hydrodynamic Workshop.

[4] Kormaz, B., K., (2015), "CFD Predictions of Resistance and Propulsion for the JAPAN Bulk Carrier (JBC) with and without an Energy Saving Device", PhD, Chalmers University.

[5] Queutey, P., Guilmineau, E., Visonneau, M., Guilmineau, E. and Deng, G. (2016), "RANS and Hybrid RANS-LES simulations around the Japan Bulk Carrier of the Tokyo 2015 CFD Workshop", Tokyo 2015 CFD Workshop. "A Workshop on CFD in Ship Hydrodynamics", National Maritime Research Institute, Tokyo, 2-4 December 2015.

[6] Catalano P. and Amato, M. (2003), "An Evaluation of RANS Turbulence Modeling for Aerodynamics", Aerospace Science and Technology 7, 2003, pp. 493-509.

[7] Menter, F.R., Matyushenko, A. and Lechner, R., "Development of a Generalized k-ω (GEKO) Two-Equation Turbulence Model", presented at the 21st DGLR-Fach-Symposium der STAB, Darmstadt, Germany, 2018 (proceedings in progress).

[8] Tracey, B., Duraisamy, K., and Alonso, J.A, (2015): "Machine Learning Strategy to Assist Turbulence Model Development",Proc. AIAA SciTech, Kissimmee, FL2015.

[9] Abdel-Malsoud M. (2019): "Experimental PIV data taken at TUHH for the twin hull JBC configuration" , Personal Communication.

[10] Large low-speed wind tunnel facilities at TUHH (Hamburg University of Technology) (https://www.tuhh.de/fds/experimental-and-computing-facilities/wind-tunnel.html).

[11] Driver, D.M., (1991): "Reynolds Shear Stress Measurements in a Separated Boundary Layer Flow", AIAA 22nd Fluid Dynamics, Plasma Dynamics and Laser Conference, AIAA-91-1787